# SWIMMING ENERGETICS OF THE LARVAL ANCHOVY, *ENGRAULIS MORDAX*

WILLIAM J. VLYMEN III[1]

## ABSTRACT

A modification of Gray and Hancock's theoretical method for studying propulsion of spermatozoa was used to estimate the energy expenditure of swimming anchovy, *Engraulis mordax*, larvae. Wave parameters obtained from photographs of feeding anchovy larvae were incorporated into a time dependent sinusoidal body displacement function which is used in the iterated energy integrals of the model. The integrals were numerically evaluated by 2-dimensional 16-point Gaussian-Legendre quadrature. The results for the mean larval length of 1.4 cm was 144.8 ergs/swimming excursion or $4.91 \times 10^{-3}$ cal/h using known excursion rates. $O_2$ consumption measurement of similar size larvae indicate a $2.19 \times 10^{-2}$ cal/h requirement. Extension to other larval sizes can be made using this model with certain qualifications. The relationships of swimming energetics to larval fish behavior are discussed. Current theories of large amplitude intermittent swimming are also discussed in light of the high swimming efficiencies encountered in this study.

The theoretical evaluation of swimming fish energetics by hydrodynamic analysis has been an extensively treated subject in recent years. Most of these treatments however have concentrated on calculation of thrust and thrust efficiencies with the exception of Lighthill (1970, 1971) who gave direct estimates for the mean swimming work rate and has drawn attention to the importance of the accelerative, virtual mass contributions in estimates of mean swimming work rate. Most expositions, however, deal with situations where inertial effects predominate with all subsequent derivations being consistent with that assumption (Taylor, 1952a). The low Reynolds number range of swimming energetics primarily of spermatozoa, has also been extensively treated (Taylor, 1951, 1952b; Gray and Hancock, 1955; Carlson, 1959; Holwill and Miles, 1971). All these treatments disregard inertial and accelerative effects in comparison with viscous effects in their treatment. Also, both viscous and inertial treatments calculate or estimate the mean swimming work rate after steady motion has been established.

The problem attacked in this paper is a synthesis and extension of the two classes of treatments discussed above, specifically to determine the energy expended per excursion by the 1-cm larval anchovy, *Engraulis mordax*. The term excursion as used here requires some elaboration. Larval anchovies have a peculiar swimming behavior because they do not continuously propagate caudally directed waves. In the adult form this behavior is noticeable by observing the tail, i.e., it does not beat continuously even though the fish appears to maintain constant forward motion. In the larval stages, however, this behavior results in an obvious discontinuous motion. The result is a series of bursts of motion from rest to rest which hereafter I refer to as excursions.

The estimation of excursion energetics by a theoretical model rather than indirect metabolic estimators during excursions is demanded because of the small size of the organisms considered, their discontinuous motion, and the investigator's inability to determine which fraction of the total energy consumption is due to swimming alone.

The parameters used in the model to calculate the excursion energy are taken from photographs of a larval anchovy of a specified size executing excursions in search of prey organisms. Since the search for prey constitutes a large proportion of the larva's activity, following Kerr (1971) we can write the total metabolism of the larva as,

$$T_T = T_F + T_C + T_S$$

where $T_T$ = total metabolism
$T_F$ = cost of search for prey

[1]Southwest Fisheries Center, National Marine Fisheries Service, NOAA, P.O. BOX 271, La Jolla, CA 92037 and Scripps Institution of Oceanography, University of California, San Diego, La Jolla, CA 92037.

Manuscript accepted January 1974.
FISHERY BULLETIN: VOL. 72, NO. 4, 1974.

$T_S$ = standard metabolism
$T_C$ = internal cost of food utilization.

The growth efficiency and subsequent relations derived from $T_T$ are important in estimating fish yields in relation to standing food resources and other factors important to fisheries management. It is this larger view which gives relevance to the rather involved procedure of simply calculating one part of the value of $T_T$, namely $T_F$.

## THEORY

The derivation of the excursion energy estimate is based on Gray and Hancock's (1955) development for spermatozoa. Instead of a cylinder with an inert head attached, the anchovy larva is regarded here as a ribbon or plate of specified width attached to an inert head (Figure 1). The assumption that the body is a ribbon is justified only if the ratio of the width to thickness ($W/t$) is $\gg 1$. In the larvae examined in this study this ratio averaged 2.5. While this ratio is not $\gg 1$ I have assumed that it is to simplify the problem. However, the error introduced is, I believe, minimal.

From Figure 1 the following relation is noted and will be used in the following derivations:

$$V_N = V_y \cos\theta - V_x \sin\theta \quad (1)$$

$$V_T = V_y \sin\theta + V_x \cos\theta \quad (2)$$

where $V_N$ = normal velocity of an element of body
$V_T$ = tangential component
$V_y$ = $y$-component
$V_x$ = $x$-component.

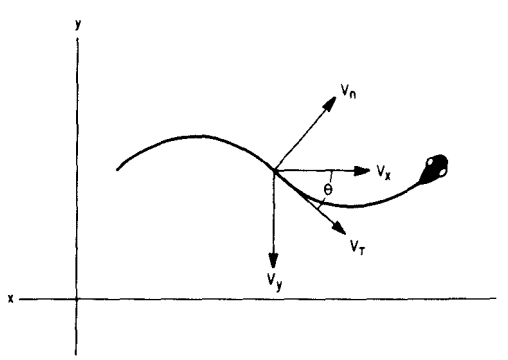


FIGURE 1.—Diagram illustrating the relationship of the velocity components of an element of body when moving transversely in the X-direction.

With the body approximated as an inextensible ribbon we find the use of the normal drag coefficient, $C_N$, and the tangential drag coefficient, $C_T$, convenient in addition to an appropriate sagittal contour function $h(s)$ where $s$ denotes distance along the spine of the fish (see Figure 4).

The expression for the velocities $V_N$ and $V_T$ is first expressed in terms of the function which represents the propagated wave along the body $y(x,t)$, and $V_x$. By noting,

$$V_y = \frac{dy}{dt} \text{ and } \tan\theta = \frac{dy}{dx}$$

we can rewrite Equations (1) and (2) as,

$$\frac{V_N}{\cos\theta} = \frac{dy}{dt} - V_x \frac{dy}{dx} \text{ and } \frac{V_T}{\cos\theta} = \frac{dy}{dt}\frac{dy}{dx} + V_x.$$

$$\text{Given } \cos\theta = \frac{1}{[1 + \tan^2\theta]^{1/2}} = \frac{1}{\left[1 + \left(\frac{dy}{dx}\right)^2\right]^{1/2}}$$

$$\text{we get } V_N = \left[\frac{dy}{dx} - V_x \frac{dy}{dx}\right]\left[1 + \left(\frac{dy}{dx}\right)^2\right]^{-1/2} \quad (1')$$

$$V_T = \left[\frac{dy}{dt}\frac{dy}{dx} + V_x\right]\left[1 + \left(\frac{dy}{dx}\right)^2\right]^{-1/2} \quad (2')$$

Now we may proceed to write the contributions to the total work of excursion made by the head, body viscous reactive terms, and accelerative body virtual mass.

The element of work performed in moving the inert head is given by,

$$dW_H = 1/2\,\rho\, C_H\, A\, V_x^3\, dt + (m + M)\frac{dV_x}{dt} V_x\, dt$$

(Vlymen, 1970)

where $dW_H$ = element of work performed by the head
$C_H$ = drag coefficient of the head
$A$ = cross-sectional area
$m$ = virtual mass of head
$M$ = mass of head
$\rho$ = density of seawater.

Thus, given the time of excursion as $t_E$ we get,

$$W_H = 1/2\int_0^{t_E} (\rho\, C_H A\, V_x^3 + 2(m + M)\frac{dV_x}{dt} V_x)dt. \quad (3)$$

The element of work performed by the body contributed by viscous-reactive forces can be approximated using experimental values for the normal and tangential drag coefficient of a smooth plate. The choices made are

$$C_N = \frac{k_N}{Re} = \frac{20.37}{Re} \quad \text{(Hoerner, 1965)} \quad (4)$$

$$\text{and } C_T = \frac{k_T}{\sqrt{Re}} = \frac{1.328}{\sqrt{Re}} \quad \text{(Schlicting, 1960)} \quad (5)$$

where $Re$ is the appropriate Reynolds number respectively. Although these are primarily low Reynolds number approximations they are within 10% at $Re = 30$. Thus $F_N$, the normal force on a plate of frontal area $A$ is given by

$$F_N = 1/2\,\rho\, C_N V_N^2\, A.$$

Since for any position along the fish body

$$Re = \frac{2V_N h(s)}{\nu}$$

$\nu$ the kinematic viscosity, we get using $C_N$ from Equation (4) the normal force $dF_N$ on an element of body ribbon as,

$$dF_N = \frac{\rho k_N \nu}{4V_N h(s)} V_N^2\, 2h(s)\, ds = \frac{\rho}{2} k_N \nu\, V_N\, ds.$$

In a similar manner $F_T$, the tangential force on a plate of total wetted surface area $A$, is

$$F_T = 1/2\,\rho\, C_T V_T^2\, A.$$

Since the formula for $C_T$ above uses $Re = \frac{V_T l}{\nu}$ where $l$ is distance measured along the body, we get the tangential force $dF_T$ on an element of body ribbon as

$$dF_T = \frac{2\rho k_T \sqrt{\nu}}{\sqrt{V_T s}} V_T^2\, h(s)\, ds$$

$$= 2\rho k_T \sqrt{\nu}\, V_T^{3/2} \frac{h(s)}{\sqrt{s}}\, ds. \quad (7)$$

Multiplying each element of force above by the element of distance in the direction of that force and summing yields,

$$dW_B^{V.R.} = \frac{\rho}{2} k_N \nu V_N^2\, dsdt + 2\rho k_T \sqrt{\frac{\nu}{s}} V_T^{5/2}\, h(s)\, dsdt$$

where $dW_B^{V.R.}$ is the element of viscous reactive work performed by an element of body ribbon. Using the Equations (1′) and (2′) for $V_N$ and $V_T$ and integrating over the excursion time $t_E$ and projected body length excluding the head we get,

$$W_B^{V.R.} = \frac{\rho}{2}\int_0^{t_E}\int_{l_H}^{l} \left[\frac{k_N \nu \left[\frac{dy}{dt} - V_x \frac{dy}{dx}\right]^2}{\left[1 + \left(\frac{dy}{dx}\right)^2\right]^{1/2}}\right] dsdt + \rho\int_0^{t_E}\int_{l_H}^{l} \frac{2k_T\sqrt{\nu}\left[\frac{dy}{dt}\frac{dy}{dx} + V_x\right]^{5/2} h(s)}{\sqrt{s}\left[1 + \left(\frac{dy}{dx}\right)^2\right]^{3/4}} dsdt.$$

where $l_H$ is the $x$-projected length of the inert head. Eliminating $ds$ by the relation,

$$ds = \left[1 + \left(\frac{dy}{dx}\right)^2\right]^{1/2} dx$$

yields finally,

$$W_B^{V.R.} = \frac{\rho}{2}\int_0^{t_E}\int_{l_H}^{l} \left[\frac{k_N \nu \left[\frac{dy}{dt} - V_x \frac{dy}{dx}\right]^2}{\left[1 + \left(\frac{dy}{dx}\right)^2\right]^{1/2}}\right] dxdt + \rho\int_0^{t_E}\int_{l_H}^{l} \frac{2k_T\sqrt{\nu}\left[\frac{dy}{dt}\frac{dy}{dx} + V_x\right]^{5/2} h(s)}{\sqrt{s}\left[1 + \left(\frac{dy}{dx}\right)^2\right]^{3/4}} dxdt.$$

As will be noted $s$ is present in the second of the

integrals above; however, later in the discussion $s$ and $h(s)$ will be converted to appropriate functions of $x$ and $t$ so that the integrations may be performed.

The accelerative or virtual mass element of work can be calculated using the fact that the virtual mass of a flat plate accelerating parallel to its normal vector is equal to the mass of the fluid enclosed in a circumscribing cylinder having the plate chord as diameter (Fung, 1969). Hence from Figure 2 the virtual mass is given by

$$dM = \rho \pi h^2(s)\, ds$$

and the magnitude of the acceleration by

$$a \sin \theta_1 = a \sin(\theta - \theta_2)$$

where $a = \left| \tilde{a} \right|$.

Now $\theta = \tan^{-1} \frac{dy}{dx}$ and $\theta_2 = \tan^{-1} \frac{V'y}{V'x}$

where $V'y = \frac{dVy}{dt}$ and $V'x = \frac{dVx}{dt}$, giving

$$a \sin(\theta - \theta_2) = a \sin\left(\tan^{-1} \frac{dy}{dx} - \tan^{-1} \frac{V'y}{V'x}\right)$$

Since $\left| \tilde{a} \right| = \left( V'^2_y + V'^2_x \right)^{1/2}$, we get

$$a \sin(\theta - \theta_2) = \left( V'^2_y + V'^2_x \right)^{1/2} \cdot \sin\left( \tan^{-1} \frac{dy}{dx} - \tan^{-1} \frac{V'y}{V'x} \right)$$

Thus the magnitude of force $F_{V.M.}$ on an element of body ribbon due to induced mass $dM$ is

$$\left| F_{V.M.} \right| = a\,dM = \rho \pi h^2(s)(V'^2_y + V'^2_x)^{1/2} \cdot \sin(\tan^{-1} \frac{dy}{dx} - \tan^{-1} \frac{V'y}{V'x}).$$

Since the element of work is given by

$$dW = \left| F_{V.M.} \right| \cdot \left| dx \right| \cdot \cos(F_{V.M.} \left| dx \right)$$

where

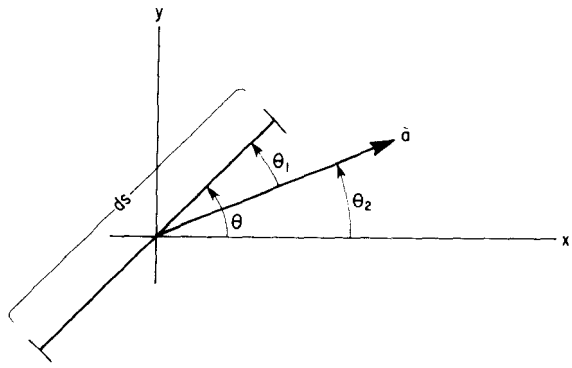


FIGURE 2.—Diagram illustrating body element undergoing acceleration $\tilde{a}$ and relationships of orientation of element to vector $\tilde{a}$ in terms of the angles $\theta$, $\theta_1$, $\theta_2$.

$$\left| dx \right| = (V^2_y + V^2_x)^{1/2}\, dt$$

and

$$\cos(F_{V.M.} \left| dx \right) = \cos(\tan^{-1} \frac{V'y}{V'x} - \tan^{-1} \frac{Vy}{Vx}),$$

we get finally

$$dW = \rho \pi h^2(s)\,(V^2_y + V^2_x)^{1/2} \quad (V'^2_y + V'^2_x)^{1/2} \cdot \sin\left( \tan^{-1} \frac{dy}{dx} - \tan^{-1} \frac{V'y}{V'x} \right) \cdot \cos\left( \tan^{-1} \frac{V'y}{V'x} - \tan^{-1} \frac{Vy}{Vx} \right) ds\,dt.$$

Using the identities for $\cos(a - b)$, $\sin(a - b)$, and $ds$ gives finally,

$$dW^A_{B_I} = \frac{\rho \pi h^2(s) \left[ \frac{dy}{dx} V'x - V'y \right] \left[ V'x\ Vx + \frac{dy}{dt} \frac{d^2y}{dt^2} \right] dx\,dt}{\left[ V'^2_x + \left( \frac{d^2y}{dt^2} \right)^2 \right]^{1/2}}$$

where $dW^A_{B_I}$ is part I of the element of work performed by the acceleration of the surrounding fluid.

In addition to $dW^A_{B_I}$ above we also want the work done in accelerating the body itself. Calling $\rho_B(s)$ the linear mass density of the body we get, using Figure 2,

$$dW^A_{B\,II} = \rho_B(s)\left(V'^2_x + \left(\frac{d^2y}{dt^2}\right)^2\right)^{1/2} \cdot \left(V^2_x + V^2_y\right)^{1/2} \cdot \cos\left(\tan^{-1}\frac{V'_y}{V'_x} - \tan^{-1}\frac{V_y}{V_x}\right) dsdt$$

where $\left(V'^2_x + \left(\frac{d^2y}{dt^2}\right)^2\right)^{1/2} = |a|$,

$\left(V^2_x + V^2_y\right)^{1/2} dt = |dx|$,

$\rho_B(s)\, ds = dm$.

When the above terms are expanded we get, taking account of $ds$,

$$dW^A_{B\,II} = \rho_B(s)\left(Vx\, V'x + \frac{dy}{dt}\frac{d^2y}{dt^2}\right)\left(1 + \left(\frac{dy}{dx}\right)^2\right)^{1/2} dxdt.$$

Integrating $dW^A_{B\,I} + dW^A_{B\,II}$ from 0 to $t_E$ in $t$ and $l_H$ to $l$ in $x$ we get the accelerative body work,

$$W^A_B = \int_0^{t_E}\int_{l_H}^{l} \rho_B(s)\left(Vx\, V'x + \frac{dy}{dt}\frac{d^2y}{dt^2}\right)\left(1 + \left(\frac{dy}{dx}\right)^2\right)^{1/2} dsdt \qquad (8)$$

$$+ \rho\int_0^{t_E}\int_{l_H}^{l} \pi h^2(s)\frac{\left[\frac{dy}{dx}V'x - V'y\right]\left[Vx\, V'x + \frac{dy}{dt}\frac{d^2y}{dt^2}\right]}{\left[V'^2_x + \left(\frac{d^2y}{dt^2}\right)^2\right]^{1/2}} dxdt.$$

The total work estimated per excursion is then given by the sum of $W^A_B$, $W^{V.R.}_B$, and $W_H$.

## METHODS

Motion picture photographs (16 mm, 128 fps) of swimming and feeding anchovy larvae were used to ascertain the various parameters in the proposed body displacement function $y(x, t) = A(t) \sin\frac{2\pi}{\lambda(t)}(x + \frac{dx_w}{dt}t)$ where $A(t)$ is the wave amplitude of the propagated wave, $\lambda(t)$ the wavelength and $x_w(t)$ the wave position as functions of time. Because of the intermittent character of the motion, variance with $x$ was not considered as important an independent variable as $t$ in the various functions comprising $y(x, t)$. The above displacement function is a general time dependent analogue of the function chosen in Holwill and Miles (1971).

The motion pictures used were obtained from John Hunter of the Southwest Fisheries Center, National Marine Fisheries Service, NOAA, and the techniques used in obtaining them are described fully (Hunter, 1972). The particular sequences used were of fish larvae varying in length from 1.2 to 1.7 cm standard length. All sequences were analyzed starting with the larvae at rest through the sine-wave execution and subsequent forward movement to rest again. The $x$-axis was considered to be parallel to the direction of forward motion as monitored by a point midway between the eyes of the fish. This point was also used to monitor forward progression.

The sequences were projected with a 16-mm Kodak[2] analyst projector on an elevated stand, through a right-angle mirror onto a table enclosed with a darkened viewing hood. At the beginning of an excursion the contour of the body was outlined with a fine-point pen on heavy-duty, low-absorbance paper. Once the outline was traced, the next frame was advanced (each frame representing 1/128 of a second) until the larva came to rest again. The mean excursion time of the larvae examined was 12.9 frames. The contour sequences thus obtained were taken to be representative of the feeding-searching behavior and were used in elucidating the wave-form parameters. In addition to the wave-contour parameters, the midpoint between the eyes was monitored for use in determining $Vx$ and $V'x$.

When the above contours and position points were obtained along with the proper magnification factors derived from knowledge of the lengths of the fish in a particular film, relevant parameter values from the tracings were

[2]Reference to trade names does not imply endorsement by the National Marine Fisheries Service, NOAA.

directly measured using a set of dial calipers read to 0.01 cm.

Many of the initial sequences of an excursion when viewed with respect to the $x$-axis as defined above showed the appearance of a wave along the proximal portion of the fish while the rest of the body coincided closely to the $x$-axis. This indicated strong $x$-dependence of the amplitude in the initial portion of the excursion. However, after three frames an almost symmetrical amplitude wave was observed. Thus the amplitude in the first several frames was taken as the maximum length of the wave above the $x$-axis (Figure 3).

The wave length was taken as that length between two successive crossings of the $x$-axis by the displacement wave form. During the later part of the excursions no crossings from positive to negative were observed and at this point the wavelength was taken as twice the value from one tangent of the body on the line of motion to the other (Figure 3).

The position of the midpoint between the eyes after each frame was monitored to yield $x(t)$. Each successive movement of that reference point was recorded in the manner outlined above and the distance moved during each frame noted.

The projected length $x_p(t)$ was taken as the length between the two points representing the projection of the tail and snout tip position on the $x$-axis and was used in a manner to be described later.

The wave position $x_w(t)$ was taken as the projected length of the body from the point where $A(t)$ is measured to the snout tip (Figure 3).

The points representing the functions described above at each unit of time, i.e., one frame, were collected for 18 excursions which were randomly selected from the larval anchovy feeding films. The functions were then nondimensionalized by division by body length and plotted. The geometric form of the resulting function was then used as a guide in selecting an appropriate descriptive function. The parameters of these functional forms were then fitted by computer in the least squares sense using a nonlinear steepest descent approach (Conway, Glass, Wilcox, 1970). The graphical representation of the proposed body displacement function with the internal functions fitted in this manner was found to coincide very closely with the actual body displacements seen in the films.

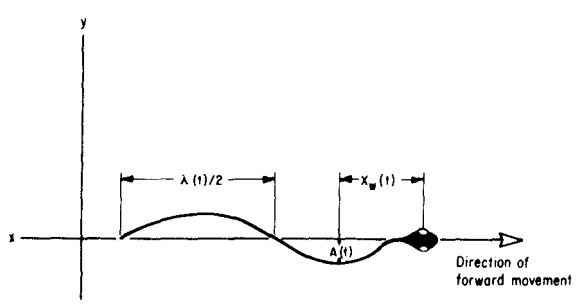


FIGURE 3.—Diagram illustrating the identification of $(t)/2$, $X_w(t)$ and $A(t)$ from photographic records (see text).

In the derivations for total excursion work, $W_T$, the integral for tangential viscous reactive work contains $s$, the distance along the fish body, explicitly. The function satisfying $F(x, t) = s$ is extremely complicated for the complete wave-form displacement function using all the fitted internal functions and is almost impossible to calculate explicitly. The alternative used here is to extrapolate back from the measured $x_p(t)$ to yield $s\ (x, t)$.

We know the function $F(x, t) = s$ satisfies

$$F(x_p, t) = L$$

where $L$ is the length of the fish body. Since the maximum amplitude ever encountered in this study was around $0.2\ L$ and the mean integration distance never greater than $\pi/2$, we can calculate, for purposes of comparison, the differences between the true length of a pure sine wave of amplitude $A$ and its projected length.

The unperturbed or no sine-wave form for a $\pi/2$ interval of integration yields simply $\pi/2$. The sine-wave projected length is, for $y = A \sin\theta$,

$$s = \int_0^{\pi/2} \sqrt{1 + A^2 \cos^2\theta}\, d\theta$$

$$= \sqrt{1 + A^2}\ E\left(\pi/2, \frac{A}{\sqrt{1 + A^2}}\right)$$

where $E(\Phi, k)$ is the elliptic integral of the second kind (in this case a complete elliptic integral of the second kind). Taking $\lambda \approx 2.0$ cm we get using $A = 0.2L$.

$$s = \sqrt{1 + 0.16}\ \ E(\pi/2, 0.37) = 1.625.$$

The difference between this and $\pi/2$ is about 4%. Thus, we expect the projected length and real body length to differ only slightly. With this confidence we make the following additional assumptions:

$$F(\lambda x_p, t) = \lambda L. \qquad \lambda \leq 1$$

This assumption based on the error calculation above postulates a linear relation between projected length and real length. Now $x_p/L = x_p(t)$ and is obtained from excursion analyses. We can rewrite this as

$$\frac{x_p}{x_p(t)} = L$$

$$\frac{\lambda x_p}{x_p(t)} = \lambda L \qquad \lambda \leq 1$$

$$\frac{x}{x_p(t)} = s \qquad x \leq x_p$$

Thus we chose to identify

$$F(x, t) = x/x_p(t) = s(x, t).$$

The determination of the contour $h(s)$ was made using biologically accurate drawings of a 1.84-cm anchovy larva. The term $h(s)$ was established for the body distal to a vertical line tangent to the gill plate as shown in Figure 4.

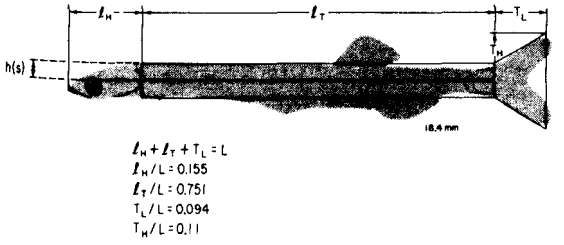


FIGURE 4.—Lateral cross section of 1.84-cm anchovy larvae displaying relationship of idealized contour function $h(s)$ (see text) to appropriate nondimensionalized morphometric parameters.

From that point to the beginning of the tail $h(s)$ was taken as a constant and the relation $h(s) = 0.038\,L$ was found to hold. The dorsal and anal fin contributions were neglected because the plate approximation already constitutes an upper bound estimate for $W_T$. Thus, the neglect of these fins quantitatively yields a more realistic estimate of $W_T$. Using the notation of Figure 4 we have,

$$h(s) = 0 \text{ for } s \leq l_H$$

$$h(s) = 0.038\,L \text{ for } l_H < s \leq (l_H + l_T)$$

$$h(s) = 0.038\,L + \frac{(T_H - 0.038\,L)}{T_L}[s - (l_H + l_T)]$$

$$\text{for } (l_H + l_T) < s \leq L$$

or using values in Figure 4 the last relation may be written

$$h(s) = 0.038L + 0.766\,(s - 0.906L).$$

The cross-sectional area $A_H$ which appears in the work integral for the head was determined by randomly selecting Formalin-preserved anchovy larvae from 0.5 to 1.5 cm in length and affixing them, via the Formalin surface tension on their bodies, upright on the side of a small inverted beaker. The largest cross section of the head was then viewed directly with a Nikon optical comparator and an outline traced from the lighted viewing screen. Lengths of the bodies were also measured with dial calipers at the time the tracings were made. Subsequently the tracing areas were measured with a planimeter and corrected to the true value. A least squares analysis of the results yielded the relation $A_H = 0.00423L^{1.23}$ where $L$ is in centimeters and $A_H$ is in square centimeters. The graph is plotted along with the data in Figure 5.

The representation for $\rho(s)$, the linear density of the body, was regarded as constant for any given length and calculated from data in Lasker, et al., (1970). Assuming 90% water, the wet weight of 0.5- to 1.6-cm larvae is then given by $0.00319L^{2.3237} = \rho(s)$ where $L$ is in centimeters and $\rho(s)$ is in grams per centimeter.

The density of the seawater was taken for $T = 17°C$ and was 1.02454. This value was obtained from tables published by the U.S. Navy Hydrographic Office (1956).

In my formulation I assume that the head is propelled through the water as an inert object attached to an undulating body. We want to know the virtual mass and drag coefficient of the inert head for use in the $W_H$ integral. Since the shape of the anchovy larva's head is

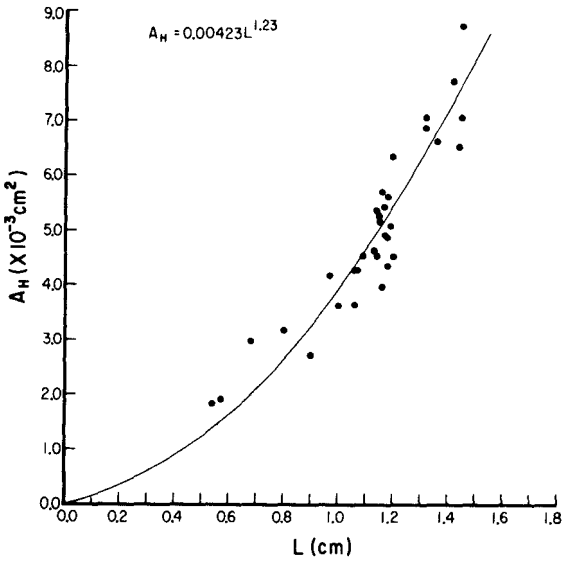


FIGURE 5.—Cross sectional area of larval anchovy head, $A_H$, as a function of length $L$.

roughly ellipsoidal or a bluff body, I decided to modify, with due consideration for the geometric differences, the drag relationship observed for a copepod (*Labidocera trispinosa*), which is a naturally occurring bluff body of similar shape, to represent the relevant characteristics of the anchovy larvae head.

If the copepod is taken as an equivalent ellipsoid, we get, from data in Vlymen (1970),

$$\overline{\left(\frac{a_c}{b_c}\right)} = 2.9$$

where $a_c$ is the major axis length and $b_c$ is the semimajor axis length of the copepod *L. trispinosa* and is given respectively by $a_c = \frac{L_c}{2}$ (one-half the metasome length) and $b_c = \left(\frac{A_H}{\pi}\right)^{1/2}$. For the anchovies studied $\frac{l_H}{L} = 0.155$ (Figure 4) and for $\bar{L} = 1.4$ cm and $A_H = 0.007$ cm$^2$, $l_H = 0.217$ cm yielding $\overline{\left(\frac{a_a}{b_a}\right)} = 2.3$.

For high Reynolds numbers ($\sim 10^4 - 10^5$) and rotationally symmetrical bluff bodies of various $l/d$ ratios, where $l$ is the bluff body length and $d$ is diameter, we have

$$\frac{C_D}{C_f} = 3\left(\frac{l}{d}\right) + 4.5\left(\frac{d}{l}\right)^{1/2} + 21\left(\frac{d}{l}\right)^2$$

(Hoerner, 1965)

where $C_f$ is the frictional drag coefficient based on wetted surface area and $C_D$ is the drag coefficient based on frontal area. We can use this relation to approximate $\frac{C_D\,(\bar{l}/d = 2.9)}{C_D\,(\bar{l}/d = 2.3)}$ assuming $C_f(l/d = 2.9) \cong C_f(l/d = 2.3)$, and use the above ratio to modify the measured drag relation already obtained for the copepod. Substituting $l/d = 2.9$ and $l/d = 2.3$ into the relation for $C_D/C_f$ we get on dividing

$$\frac{C_D\,(l/d = 2.9)}{C_D\,(l/d = 2.3)} = 1.00.$$

At lower Reynolds numbers we expect the geometric differences to cause a greater discrepancy between $C_D\,(l/d = 2.9)$ and $C_D\,(l/d = 2.3)$. In particular $C_D\,(l/d = 2.9) > C_D\,(l/d = 2.3)$. However, since in my experiments $Re$ was from 0- to 100, the region where we expect the $C_D\,(Re)$ curve to flatten out to a fairly constant value we take $C_D\,(Re)$ for the copepod as a first approximation to the $C_D\,(Re)$ for the anchovy head. That function is $C_D\,(Re) = 85.2/Re^{.80}$, Vlymen (1970). The virtual mass, $m$, occurring in the integrals for $W_H$ is then calculated by considering the head as if it were an equivalent ellipsoid. Using $(a_a/b_a) = 2.3$ we can calculate $m$ as $m = k_1 \rho V_D$ where $k_1 = \frac{\gamma}{(2-\gamma)}$

$$\gamma = 2\left(\frac{1-\epsilon^2}{\epsilon^3}\right)\left[1/2 \log\left(\frac{1+\epsilon}{1-\epsilon}\right) - \epsilon\right]$$

$$\epsilon = \left(1 - \frac{b_a^2}{a_a^2}\right)^{1/2}$$

$V_D = 4/3\,\pi a_a b_a^2$ Vlymen (1970).

For a 1.4-cm larva $m$ has a value of $1.80 \times 10^{-4}$ g and assuming the head density is the same as seawater we get $M = 7.9 \times 10^{-4}$ g. Thus $W_H$ may be rewritten as

$$W_H = 1/2 \int_0^{t_E} 85.2\left(\frac{\nu}{L}\right)^{.80} V_x^{2.2} A_H\, dt$$

$$+ \int_0^{t_E} (9.7 \times 10^{-4} \frac{dV_x}{dt} V_x\, dt$$

where $\nu$ is the kinematic viscosity of seawater 0.0119 $cm^2$–$s^{-1}$ (U.S. Navy Hydrographic Office, 1956).

A computer program by Stroud (1971) using 16-point Gauss-Legendre integration, and the above outlined integration scheme was used to compute the integrals comprising $W_T$. The program was translated into Algol and executed on a Burroughs 6700 at the University of California, San Diego Computer Center. Accuracy of the program was checked by evaluation of the iterated integrals

$$\int_0^w e^{-y^2}\,dy \int_0^y e^{x^2}\,dx \text{ for various } w \text{ and}$$

$$\int_0^1 \int^{\sqrt{1-x^2}} \sqrt{1-x^2-y^2}\,dy\,dx = \frac{\pi}{6}.$$

The results showed the integration scheme to be accurate to the eighth decimal place in the former integral when compared with tables in Rosser (1948) and accurate to the fourth decimal place in the latter integral using standard tables. Details of the mathematical scheme are found in the appendix.

In the integrations of $W_T$ a relative convergence was computed by first doing the integration over the whole interval, that is,

$$I_0 = \int_0^t \int_{f(t)}^{g(t)} F(x, t)\,dxdt.$$

Then the value corresponding to one subdivision is computed, namely,

$$I_1 = \int_0^{t/2} \int_{f(t)}^{g(t)} F(x, t)\,dxdt + \int_{t/2}^{t} \int_{f(t)}^{g(t)} F(x, t)\,dxdt.$$

The relative convergence is then computed as

$$C = \frac{I_1 - I_0}{I_1}.$$

If this value is less than 0.05, the value $I_2$ is taken as the value of the integral. If it is greater, the intervals comprising $I_2$ are further subdivided and the process continued until convergence is reached. Thus, if $I_n$, corresponding to $2^n$ subdivisions, and $I_{n+1}$, corresponding to $2_{n+1}$ subdivisions, are of such values that

$$\frac{I_{n+1} - I_n}{I_{n+2}} < 0.05,$$

then $I_0$ is assigned the value $I_{n+1}$.

The convergence is set higher than one might expect because computation of the complex integrals of the type used in this study is manifested by slow and oscillatory relative convergences necessitating a great deal of computer time. However, when the convergence criteria was set at 0.05 in the integrations performed, convergences were better than the critical value. The effect of the higher convergence criteria is thus seen as being an economic and computational convenience.

## RESULTS

The plotted values of the nondimensional amplitude, $A(t)/L$, wave position, $X_w(t)/L$, and projected length, $X_p(t)/L$, along with the descriptive functions fitted by the methods discussed are shown in Figures 6 and 7. The points comprising the curves of each represent the mean value of the particular parameter in question at successive units of time where one time unit is $^1/_{128}$ s.

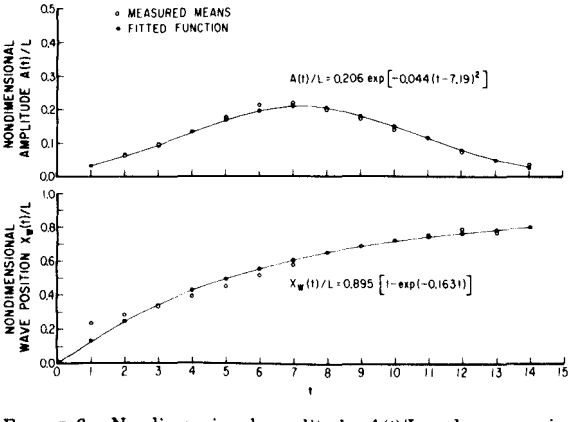


FIGURE 6.—Nondimensional amplitude, $A(t)/L$ and wave position, $X_w(t)/L$, of body displacement function as functions of time, $t$, in motion frame units. The graphs display the fitted curves (line) together with the original data (open circles) and points of the fitted curve at corresponding time units (closed circles).

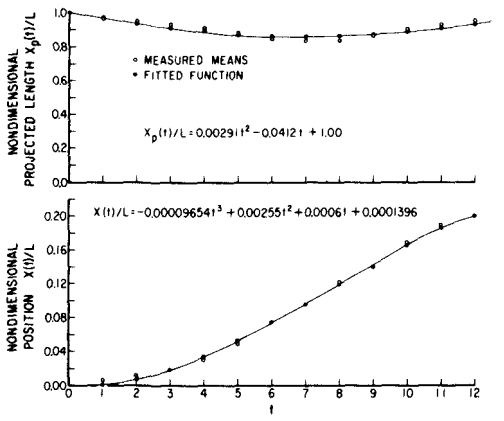


FIGURE 7.—Nondimensional position, $X(t)/L$, and projected body length, $X_p(t)/L$, as functions of time, $t$, in motion frame units. The graphs display the fitted curves (lines) together with the original data (open circles) and points of the fitted curve at corresponding time units (closed circles).

The curve for $\lambda(t)/L$, deserves some discussion. Since the amplitude of the propagated wave was known to be zero at $t = 0$, both $\lambda = \infty$ or $\lambda = 0$ would be descriptive of the initial straight-line configuration. However, $\lambda = 0$ implies an infinite number of oscillations varying like sin $t/\lambda$ with neither the function nor the first derivative existing as $\lambda \rightarrow 0$. Since at the end points of an excursion a slightly perturbed wave form was observed, i.e., a finite wavelength, the nondimensional wavelength of the $t = 0$ excursion wave form was adjusted to be equal to the last. A perfect relation

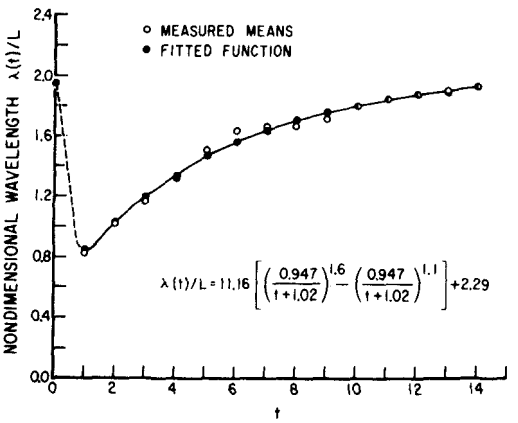


FIGURE 8.—Nondimensional wavelength, $\lambda(t)/L$, as a function of time, $t$, in motion frame units. The graph displays the fitted function (line) together with the original data (open circles) and points of the fitted curve at corresponding time units (closed circles). The dotted portion of the fitted curve is discussed in the text.

would have $\lambda = \infty$ at both end points. This, I believe, does not drastically affect the results since the only modulatory component at the end points is the amplitude which is zero at these points. This accounts for the Lennard-Jones type of function which was chosen as a functional representation of $\lambda(t)/L$ and is shown in Figure 8 along with the function itself. The values at other than the end points together with the fact that $A(t) = 0$ at these points is sufficiently descriptive of the contour wavelength to vitiate any physical inconsistencies or mathematical problems that may arise from the end point modification of $\lambda(t)/L$ discussed.

The integrals representing the work per excursion namely $W_B^{V.R.}$, $W_B^A$, $W_H$ were subdivided further into smaller iterated integrals and, using the mean excursion time of 12.9 frame time units (~0.10s) integrated by the method already outlined. The values obtained were taken to represent the work/excursion of an anchovy larvae of length equal to the mean of the animals used in the study or 1.4 cm.

The values of the work are divided into five categories as follows: 1) head energy representing the value of the integral in Equation (3), 2) normal energy representing the value of the 1st integral of $W_B^{V.R.}$, 3) tangential energy representing 2nd integral of $W_B^{V.R.}$, 4) body inertial energy representing the 1st integral of $W_B^A$, and 5) inertial energy representing the 2nd integral of $W_B^A$. The value of these five integrals in ergs/excursion and their fraction of the total excursion energy is given in Table 1. It is observed from the table that accelerative terms such as body inertial and inertial energies account for more than three-fourths of all the energy used in swimming. It is worthwhile noting that although this is an expected outcome of the peculiar behavior of the anchovy larvae, it is possibly true that neglect of such terms in many analyses of fish energetics is cause for errors. Attention to these matters has been given thorough theoretical discussion in Lighthill (1970, 1971). The analysis in this paper,

TABLE 1.—Excursion energy components in ergs for the 1.4-cm anchovy larva.

| Item | Energy/ excursion | Percent of total |
|---|---|---|
| Normal energy | 11.5 | 7.9 |
| Tangential energy | 0.35 | 0.2 |
| Inertial energy | 33.6 | 23.2 |
| Body inertial energy | 99.2 | 68.5 |
| Head energy | 0.15 | 0.2 |
| Total energy | 144.8 | |

however, depends on incorporating what actually occurs into an easily manipulated theoretical energy construct.

Although the point of this study is to evaluate the swimming energetics in an indirect but nonmanometric manner, it is nevertheless interesting to compare the calculated energy using the theoretical model with values obtained using $O_2$ consumption measurements obtained with anchovy larvae. Such experiments in limited numbers have been performed by Lasker (pers. commun.) using more than one larva per experiment and with the animals confined to small volume containers. No knowledge of activity levels was possible during these experiments and the values obtained reflect total $O_2$ uptake per experimental period averaged for the number of larvae per container. Lasker believes, however, that activity levels during such experiments are below natural levels because of the inhibiting effects of the container surfaces and crowding. The value obtained from such experiments was $4.36 \pm 1.05$ $\mu$l $O_2$/mg dry wt/h. Assuming an $RQ$ of 0.70 we get 1 $\mu$l $O_2$ = 0.005 cal $\pm$ 0.00035 (Lasker, 1962). Thus, the caloric equivalent of the anchovy larval respiratory rate is between 0.0153 cal/mg dry wt/h and 0.0289 cal/mg dry wt/h with a mean value of 0.0218 cal/mg/h ($n$ = 23). A comparison between the theoretically determined energy value and the mean $O_2$ uptake value given above requires a simultaneous knowledge of swimming activity expressed as an excursion frequency. Such information is not available and it is precisely our inability to make simultaneous observations of $O_2$ consumption and activity of fish larvae that necessitates the type of study undertaken in this paper. Excursion rates observed during 5-min feeding-searching periods have been measured (Hunter, 1972) using large containers. For the periods observed the excursion rate appropriate to a 1.4-cm larvae was found to be $1.57 \pm 0.03$ excursions/s with the mean time devoted to intermittent swimming being $82.6\% \pm 1.2\%$. This value is probably a maximum for activity since satiation would probably lead to a decrease in excursions as would the lack of observable food particles. Since available $O_2$ measurements were not collected during feeding, some modification of the above activity value has to be made to compensate for the inhibition of the container and the absence of food before these values can be used for comparison.

The $O_2$ consumption measurements of anchovy larvae were performed in small 70-ml containers in light and darkness. The only relative activity measurements that have been performed for similar situations were on 28-day-old herring larvae ca. 1 cm in length in a variety of light conditions by Blaxter (1973). Although herring are continuous swimmers, unlike anchovy larvae, the use of relative activities was deemed an appropriate way of estimating the activity variation of a similar sized nonfeeding organism in the following manner. For herring larvae at 10 different light levels the mean percent difference between maximum and mimimum activity levels was found by Blaxter (1973) to be 78.6%, maximum activity being defined as mean activity plus two standard errors and minimum activity as mean activity minus two standard errors. Although this change is large, it probably reflects behavioral modulation more than effects of the container since in Blaxter's experiment the container (a long tube) contained approximately 1,500 ml of seawater. Thus, regarding the $O_2$ consumption experiments on the anchovy as representing the minimum activity levels of that organism in the same relationship of active to inactive as found from Blaxter (1973), we can, using known maximum excursion rates during feeding from Hunter (1972), calculate the minimum excursion rate or activity corresponding to our $O_2$ measurements and hence the energy consumption for swimming based on that excursion rate. This analysis assumes the geometric swimming behavior during feeding and nonfeeding is the same, an assumption confirmed by observation.

Using the mean $O_2$ consumption value 0.0218 cal/mg dry wt/h and the dry weight of a 1.4-cm larva from Lasker et al. (1970) we get an expenditure of $22.6 \times 10^{-3}$ cal/h. Taking 1.57 excursions/s as the mean maximum activity value, decreased by 78.6% to convert to minimum activity levels, and multiplied by the theoretically determined energy per excursion of the 1.4-cm larva of 144.8 ergs/excursion, we get $4.91 \times 10^{-3}$ cal/h. This value yields an estimate of metabolic swimming efficiency of 24.6% for the 1.4-cm larval anchovy assuming a poikilothermic basal metabolic rate of 0.05 $\mu$l $O_2$/mg wet wt/h. This efficiency is quite high when compared to values obtained for larger fish where efficiencies in the range of 8 to 15% (Webb, 1971) are observed. However, such experiments are usually done on large fish constrained by relatively small tanks, swimming continuously, and using a caudal propeller mode of propulsion. Thus any comparison of the above results

with the wide-range Reynolds number motions and large amplitude wave forms encountered in this study must be done cautiously and with appropriate consideration of hydrodynamical dissimilarities. However, using the most obvious behavioral differences between the two types of studies, a higher overall efficiency might be suspected based on the viewpoint of Lighthill (1971) that the large amplitude tail motions exhibited by some fishes be interpreted as a means of producing reactive thrusts which balance the enhanced viscous drag produced upon the commencement of lateral movements. Lighthill thus implies that large amplitude movements interspersed with periods of gliding are more efficient than continuous small amplitude oscillations as a mode of propulsion. This appears to be confirmed in the results of this study where the behavior is of this type and the efficiency apparently high. It should be stressed that a range of efficiencies can exist due to the intrinsic variability in $O_2$ consumption values and associated activity measurements and the fact that synchronous determinations of both have not yet been performed. The purpose of the swimming efficiency calculation and the associated comparison curves with $O_2$ values (Figure 9) is to demonstrate the relationship the theoretical values determined here have to the available physiological parameters obtained with simple experimental designs. If excursion energies could be obtained by simpler means, one could circumvent the involved procedures presented in this paper.

It is interesting to note that the Pacific sardine, *Sardinops caerulea,* whose ecological niche was primarily taken over by the anchovy, *Engraulis mordax,* in the California Current (Murphy, 1966) does not exhibit, in the larval stages, the same swimming behavior as the anchovy, i.e., swimming bursts followed by glides. Instead it swims by constant, small amplitude oscillating movements of the body. In light of the results here and theoretical work by Lighthill it is possible that the propulsive efficiencies in the larval stages of the sardine and anchovy are slightly different, the sardine being less efficient. Thus a small behavioral-propulsive difference between the anchovy and the sardine might have permitted the anchovy to compete more favorably when there was a decline in sardine population.

The evaluation of propulsive energetics as outlined in this study is directed at only one size of the anchovy larva because the method

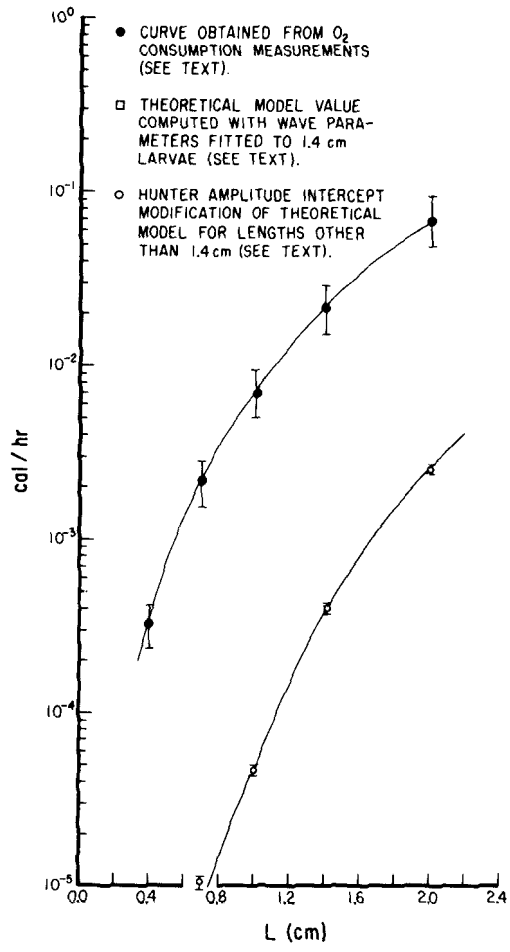


FIGURE 9.—Energy consumption of swimming based on theoretical model (open circles and open square) and total energy consumption based on $O_2$ utilization (closed circles) as a function of length. Vertical lines on both curves span one standard error of the data.

requires detailed knowledge of the various wave-form parameters as functions of time for each length of the organism studied. Valid results cannot be obtained for other sizes by a mere alteration of the length of the organism in the wave-parameter functions. By the method outlined here, the only way to properly evaluate propulsive energetic costs for different lengths would be to repeat the course of wave-parameter determination completely. However, with such limitations in mind it is interesting to compare results obtained when modification of the existing wave-parameter functions is made using extensions of known length-dependent wave-parameter quantities which have been measured for larval anchovies. The

only such wave parameter available for modification and incorporation into the energy formulation is the wave amplitude.

Hunter (1972) measured the relationship between tail-beat amplitude and larval length for intermittent swimming and found the relationship,

$$A = 0.112 + 0.170L$$

where $L$ and $A$ are in centimeters. Since minimal amplitude dependence on length exists because of the exaggerated whiplike motion of the tail, Hunter's amplitude value is greater than my value for the maximum wave amplitude of 1.4-cm larvae. This is because amplitudes used in this study are measured as the wave crest progresses caudally at each successive time unit, whereas at the tail, wave progression ceases along the body and may even become retrograde due to the whiplike motion. The important point is the intercept at zero length where both measurements must be consistent, i.e., equal. Thus, admitting equality of the interception point at $L = 0$ and adjusting the first order coefficient in Hunter's equation to yield the correct value for maximum amplitudes at $L$ = 1.4 cm we get,

$$A_{max} = 0.112 + 0.094\ L$$

This value was substituted for $A_{max} = 0.026\ L$ in the amplitude function $A(t) = 0.206\ L \exp[-0.044\ (t - 7.19)^2]$ and its first two derivatives used in the $L$ = 1.4 cm formulation. The work integrals were then recomputed at the three new points $L$ = 0.4 cm, $L$ = 0.7 cm, and $L$ = 2.0 cm. Because the $A_{max}$ values coincided at $L$ = 1.4 for both treatments this value was not used again in the integration procedure. The values obtained are shown in Table 2. Least squares regression of the data assuming the functional form $E = aL^b$ where $E$ is energy/excursion in ergs and $L$ length in centimeters yielded $E = 27.5\ L^{4.48}$. The energy/excursion calculated for the four additional lengths was then converted to hourly energy rates using the excursion frequencies cited earlier. The results obtained were plotted with scales of calories per hour vs. length in centimeters. For comparison, another curve of the form $\frac{dO_2}{dt} = f(L)$ was computed and plotted along with the curve formed using the additional model points above (Figure 9). The line shown connecting these points is fitted by eye. The comparison curve was based on the respiration value of 0.0218 cal/mg dry wt/h and the following relationship between dry weight in milligrams and length in millimeters, $\log W = 3.3237 \log L - 3.8205$ (Lasker et al., 1971). This comparison curve is isomorphic to the length-weight curve with no allowance being made for specific respiration changes with increasing weight. Therefore the curve is to be regarded as the best approximation to the total $O_2$ consumption rate for swimming larval anchovies. It provides only a means of judging the physiological reliability of the energy summation method employed here. However, because the changes in specific respiration as a function of weight would not change this comparison curve appreciably, it can probably be regarded as sufficiently reliable. With this understanding some comparison of these curves can be made.

TABLE 2.—Excursion energies for five larval anchovy lengths using Hunter's modified intercept amplitude function (see text for complete discussion) for extension to larval lengths other than 1.4 cm.

| Length (cm) | Energy/ excursion (ergs) |
|---|---|
| 2.0 | 881.4 |
| 1.4 | 144.8 |
| 1.0 | 16.3 |
| 0.70 | 3.6 |
| 0.40 | 0.76 |

From laboratory observation of larvae it seems apparent that nondimensional amplitude and wavelength do not remain constant but decrease in absolute value as length is increased. That is, functions descriptive of these nondimensional parameters do not remain descriptive of animals of all lengths. That is exactly what is observed as we deviate from the original $L$ = 1.4 cm point where the nondimensional wave parameters are fitted. Even with modification of $A_{max}$ used to compute the original curve this effect is still observable. Part of the deviation is, however, due to the behavior of the larvae as age increases. Very small larvae float 90% of the time with occasional bursts of intensive activity (Hunter, 1972) which, as I pointed out earlier, is quite inefficient. As the larvae get older, however, intermittent, more efficient swimming becomes the dominant mode of locomotion. This trend is partially reflected in these two curves. As the larvae get older and

larger the intermittent swimming rate decreases and the nondimensional amplitude and wave functions decrease also. This accounts for the large locomotion energy computed for larvae greater than 1.4-cm in length. It is interesting to note how behavioral factors, when unavoidably neglected in extending this curve, become evident when compared with reasonable estimates for total energy consumption.

In view of the behavioral-mathematical factors influencing the shape of the theoretical curve in the directions observed here and the physiologic reasonableness of the metabolic swimming efficiencies obtained when exact wave parameters descriptive of the $L$ = 1.4-cm larva are used, it is reasonable to conclude that the energies calculated from the model are the best estimates of the swimming energetic requirement per excursion of the larval anchovy, excursion being regarded as a discrete, reproducible behavioral entity, currently available.

Therefore, the major results of this study are 1) the demonstration that modifications of existing methods of computing energy of translation yield information on behavior when consideration is given to differences in behavior, shape, and flow scale, 2) that a good correlation exists in terms of metabolic swimming efficiency obtained between direct $O_2$ measurements and the model, 3) a confirmation of the high efficiency of large amplitude, intermittent swimming behavior, and 4) quantitative estimates of swimming energy requirements derived from this model may be used for other larval anchovy research.

Theoretical studies such as random walk analyses and correlations with feeding behavior and migration which are being studied currently could incorporate these data to provide a comprehensive and quantitative picture of larval anchovy energetics and behavior.

## ACKNOWLEDGMENTS

I thank Reuben Lasker of the Southwest Fisheries Center, National Marine Fisheries Service, NOAA, for proposing this study, donation of facilities, critical reading of the manuscript, and kind and constant encouragement throughout its execution. I would also like to thank John Hunter, Southwest Fisheries Center, National Marine Fisheries Service, NOAA, for numerous helpful discussions on aspects of larval behavior and loan of larval anchovy feeding films. Appreciation is also expressed to the staff of the National Marine Fisheries Service computer facility for their assistance in this project. This work was supported by NOAA, Office of Sea Grant, Department of Commerce, under grant #UCSD 04-3-158-22.

## LITERATURE CITED

ABRAMOWITZ, M., AND I. A. STEGUN (editors).
1966. Handbook of mathematical functions with formulas, graphs, and mathematical tables. National Bureau of Standards Applied Mathematics Series 55, 5th printing. Gov. Print. Off., Wash., D.C.

BLAXTER, J. H. S.
1973. Monitoring the vertical movements and light responses of herring and plaice larvae. J. Mar. Biol. Assoc. U.K. 53:635-647.

CARLSON, F. D.
1959. The motile power of a swimming spermatozoon. *In* H. Quastler and H. J. Morowitz (editors), Proceedings of the First National Biophysics Conference, Columbus, Ohio, March 4-6, 1957, p. 443-449. Yale Univ. Press, New Haven.

CONWAY, G. R., N. R. GLASS, AND J. C. WILCOX.
1970. Fitting nonlinear models to biological data by Marquardt's algorithm. Ecology 51:503-507.

FUNG, Y. C.
1969. An introduction to the theory of aeroelasticity. Dover Publ. Inc., N.Y., 406 p.

GARY, J., AND G. J. HANCOCK.
1955. The propulsion of sea-urchin spermatozoa. J. Exp. Biol. 32:802-814.

HOERNER, S.
1965. Fluid dynamic drag. Publ. by author Midland Park, N.J.

HOLWILL, M. E. J., AND C. A. MILES.
1971. Hydrodynamic analysis of non-uniform flagellar undulations. J. Theor. Biol. 31:25-42.

HUNTER, J. R.
1972. Swimming and feeding behavior of larval anchovy, *Engraulis mordax*. Fish. Bull., U.S. 70:821-838.

KERR, S. R.
1971. Prediction of fish growth efficiency in nature. J. Fish. Res. Board Can. 28:809-814.

LASKER, R.
1962. Efficiency and rate of yolk utilization by developing embryos and larvae of the Pacific sardine *Sardinops caerulea* (Girard). J. Fish. Res. Board Can. 19:867-875.

LASKER, R., H. M. FEDER, G. H. THEILACKER, AND R. C. MAY.
1970. Feeding, growth, and survival of *Engraulis mordax* larvae reared in the laboratory. Mar. Biol. (Berl.) 5:345-353.

LIGHTHILL, M. J.
1970. Aquatic animal propulsion of high hydromechanical efficiency. J. Fluid Mech. 44:265-301.
1971. Large-amplitude elongated body theory of fish locomotion. Proc. R. Soc. Lond., Ser. B, 179:125-138.

MURPHY, G. I.
1966. Population biology of the Pacific sardine (*Sardinops caerulea*). Proc. Calif. Acad. Sci., Ser. 4, 34:1-84.

ROSSER, J. B.
1948. Theory and application of $\int_0^z e^{-x^2} dx$ and $\int_0^z e^{-p^2y^2} dy \int_0^y e^{-x^2} dx$. Part I. Methods of computation. Mapleton House, Brooklyn, N.Y., 192 p.
SCHLICTING, H.
1960. Boundary layer theory. 2d ed. McGraw-Hill Book Co., N.Y., 122 p.
STROUD, A. H.
1971. Approximate calculation of multiple integrals. Prentice-Hall Inc., Englewood Cliffs, N.J.
TAYLOR, G.
1951. Analysis of the swimming of microscopic organisms. Proc. R. Soc. Lond. Ser. A, 209:447-461.
1952a. The action of waving cylindrical tails in propelling microscopic organisms. Proc. R. Soc. Lond., Ser. A, 211:225-239.
1952b. Analysis of the swimming of long and narrow animals. Proc. R. Soc. Lond., Ser. A, 214:158-183.
U.S. NAVY HYDROGRAPHIC OFFICE.
1956. Tables for rapid computation of density and electrical conductivity of sea water. H.O. (Hydrogr. Off.) Sp-11, 24 p.
VLYMEN, W. J.
1970. Energy expenditure of swimming copepods. Limnol. Oceanogr. 15:348-356.
WEBB, P. W.
1971. The swimming energetics of trout. II. Oxygen consumption and swimming efficiency. J. Exp. Biol. 55:521-540.

## APPENDIX

The integration of the iterated integrals was accomplished via a two-dimensional extension of the standard Gauss-Legendre guadrature. The one-dimensional fixed limit integration formula was used by Holwell and Miles (1971) for similar classes of functions with good results. The type of integrals requiring evaluation were of the general form

$$\int_a^b \int_{f(t)}^{g(t)} F(x, t)\, dxdt$$

$a$, $b$, fixed.

Defining

$$G(t) = \int_{f(t)}^{g(t)} F(x, t)\, dx,$$

we get

$$\int_a^b \int_{f(t)}^{g(t)} F(x, t)\, dxdt = \int_a^b G(t)dt.$$

By $n$-point Gauss-Legendre quadrature Abramovitz and Stegun (1966) this is given approximately by,

$$\int_a^b G(t)dt \cong \frac{b-a}{2} \sum_{i=1}^{n} w_i\, G(\xi_i)$$

where $\xi_i = \frac{b-a}{2}\, y_i + \frac{b+a}{2}$

$y_i$ = $i$th zero of $P_n(x)$, the $n$-order Legendre polynomial and

$$w_i = 2/\left(1 - y_i^2\right) \left[P'_n(\xi_i)\right]^2 .$$

Using Gauss-Legendre quadrature on $G(\xi_i)$ yields,

$$\int_a^b G(t)dt \cong \frac{b-a}{2} \sum_{i=1}^{n} w_i \int_{f(\xi_i)}^{g(\xi_i)} F(x, \xi_i)\, dx$$

$$\cong \frac{b-a}{2} \sum_{i=1}^{n} w_i \frac{g(\xi_i) - f(\xi_i)}{2} \sum_{j=1}^{n} w_j^* F(\eta_j, \xi_i),$$

where $\eta_j = \frac{g(\xi_i) - f(\xi_i)}{2}\, y_j + \frac{g(\xi_i) + f(\xi_i)}{2}$

$w_j^* = 2/(1 - y_j) \left[P'_n(\eta_j)\right]^2$ and

$y_j$ = $j$th root of $P_n(x)$.

We have finally the result,

$$\int_a^b \int_{f(t)}^{g(t)} F(x, t)\, dxdt \cong \frac{b-a}{2} \sum_{i=1}^{n} \sum_{j=1}^{n} w_i\, w_j^* \frac{g(\xi_i) - f(\xi_i)}{2} F(\eta_j, \xi_i),$$

where the above definitions hold.